



Reacting Flow Solver For Martian Atmosphere Conditions

P. Vicky Kumar, Anil Kumar Birru and
Vinayak Narayan Kulkarni

EasyChair preprints are intended for rapid
dissemination of research results and are
integrated with the rest of EasyChair.

January 15, 2020

Reacting Flow Solver For Martian Atmosphere Conditions

P Vicky Kumar¹, Dr.Anil Kumar Birru², Dr.Vinayak Narayan Kulkarni³

¹ Mechanical Engineering, NIT Manipur, Imphal, India, papulappa@gmail.com

² Mechanical Engineering, NIT Manipur, Imphal, India, birruresearch@gmail.com

³ Mechanical Engineering, IIT Guwahati, India, vinayak@iitg.ernet.in

Reacting Flow Solver For Martian Atmosphere Conditions

ABSTRACT

In the advancement of a computational code, demonstration depict essential element. An attempt has been made to develop finite volume inviscid non-equilibrium flow solver especially flow of carbon-dioxide to study Martian atmospheric condition. The present study utilizes Venkat Krishnan limiter to provide second order accuracy. The solver is incorporated by higher order reacting convective or inviscid fluxes, AUSM scheme. The code is inspected by flowing carbon dioxide over sphere of diameter 25.4mm and shock stand-off distance is measured at two different velocities i.e. 4.220km/s and 2.845km/s. Similarly, for ramp at angle 10 and 20 degree the results obtained in terms of pressure ratio, temperature ratio and wave angle by solver is validated with analytical approach. For all the cases studied, in house-solver exhibit satisfying agreement. Additionally, its capability can be enhanced by incorporating various flux evaluation schemes.

Keywords: Martian atmosphere, AUSM scheme, Shock stand-off distance and wave angle

1. INTRODUCTION

Martian atmosphere mainly consists of 95.70% CO₂, 1.6% Ar and 2.7% N₂ is quite different from Earth's. The density is only 1.0% and the temperature is lower than Earth's atmosphere. The atmosphere and climates in Mars vary severely and quasi-randomly with Mars geographic position and seasons, which makes the atmosphere parameters having evident scatter characteristic. As a result, these uncertainties of atmosphere parameter do not be neglected in entry vehicles aerodynamics computations in virtue of its interdependency with the trajectory design. A lot of probes supported from Mars exploration projects by U.S. and S.U during the cold war period were launched to Mars. Unfortunately, most of them were failed until the "Viking" explorer belonging to NASA successfully entered Martian atmosphere in 1976. Then, NASA's another explorer, the "Pathfinder", successfully landed Mars once again in 1996. However, contemporary Mars probes from Russia and Japan all failed for different reasons. With the development of aerospace technology and understanding the environments of Mars atmosphere, the success probability of Mar exploration mission significantly grows in 21st century, such as the well-known projects Phoenix and Mars Science Laboratory, Mars exploration attracts more and more countries concern. From the view of vehicles entry, there are still a lot of challenges, especially in accurately predicting aerodynamics characteristics concerning Martian atmosphere. Candler et al. [1] conducted an experiment in an expansion tube facility at three different angles of attack: 0, 11, and 16 deg. In a hypervelocity carbon dioxide flow were made to measure heat flux across blunt bodies and visualize bow shock shapes. White et al. [2] simulated Monte Carlo solver, known as dsmc Foam, is thoroughly examined for its ability to solve low and high speed non-reacting gas flows in simple and complicated geometries. Two test cases were considered i.e. flow over sharp and truncated flat plates, the Mars Pathfinder probe, a micro-channel with heated internal steps, and a simple micro-channel. Liao et al. [5] measure shock stand-off distances over hypersonic spheres in CO₂ have been conducted in the hypervelocity ballistic range of HAI, CARDC. It is thought from the calculated results that the flow over spheres of present test is mainly non equilibrium. Vital parameters like skin friction coefficient, mass fraction of various species, boundary layer thickness, entropy layer thickness etc. are either impossible or very difficult and costly to obtain by performing experiments. Hence, it is advisable to devise a methodology for known freestream conditions and geometry by employing finite volume inviscid non-equilibrium flow solver for investigation and to obtain more detailed flow field information.

2. NUMERICAL METHODOLOGY

2.1 Governing Equations

Computational fluid dynamic (CFD) is a methodology to solve the governing mathematical models for fluid flow using suitable numerical technique. It is an efficient approach to simulate the variety of fluid problems in an economical way as compared to costly experimental procedures. Therefore, it has been integral part of designing supersonic/hypersonic aircraft like reentry vehicles, missiles etc. Simulation for these compressible flows involves the solution of Euler's equations for low enthalpy conditions. However, consideration of

reacting gas flow is important for precise prediction of high enthalpy flowfield. Therefore, species continuity equations also need to be solved along with the Euler's equations. The source term of these added equations accounts for the species production rate which is insignificant in the low enthalpy non-reacting gas flow. The coupled Euler's equation and species continuity equations for 2-D axisymmetry laminar Inviscid compressible flows in vector form are presented as follows: -

$$\frac{\partial U}{\partial t} + \frac{\partial F}{\partial x} + \frac{\partial G}{\partial y} + S + \alpha S_I = 0$$

Where,

$$U = \begin{pmatrix} \rho \\ \rho u \\ \rho v \\ \rho E \\ C_1 \\ \vdots \\ C_{N-1} \end{pmatrix}, F = \begin{pmatrix} \rho \\ \rho u^2 + p \\ \rho uv \\ \rho E + p \\ u C_1 \\ \vdots \\ u C_{N-1} \end{pmatrix}, E = \begin{pmatrix} 0 \\ \tau_{xx} \\ \tau_{xy} \\ u\tau_{xx} + v\tau_{xy} - q_x - \sum_{i=1}^N h_i C_{iu} \bar{u}_i \\ -C_1 \bar{u}_1 \\ \vdots \\ -C_{N-1} \bar{u}_{N-1} \end{pmatrix}$$

$$G = \begin{pmatrix} \rho v \\ \rho uv \\ \rho v^2 \\ (\rho E + p)v \\ v C_1 \\ \vdots \\ v C_{N-1} \end{pmatrix}, S_I = \frac{1}{y} \begin{pmatrix} \rho v \\ \rho uv \\ \rho v^2 \\ (\rho E + p)v \\ v C_1 \\ \vdots \\ v C_{N-1} \end{pmatrix}, S = \begin{pmatrix} 0 \\ 0 \\ 0 \\ 0 \\ S_1 \\ S_2 \\ \vdots \\ S_{N-1} \end{pmatrix}$$

With total energy E, is expressed as $E = e + \frac{1}{2} \rho(u^2 + v^2)$ where used for internal energy 'e'. This internal energy of the mixture be able to calculate as, $e = \sum_{i=1}^N e_i \frac{C_i}{\rho MW_i}$. 'F' and 'G' denotes flux in vector form in x and y direction along with 'U' as conservative vector or solution, respectively. 'S' denotes reaction source term and 'S_I' called axisymmetric source term. When 'α' is assigned as 1 and 0, it recognizes axi-symmetric and 2-D simulation. Additionally, ρ, p and T represent density, pressure and temperature. Whereas u and v are velocities in x and y direction respectively. The molar internal energy of the species is calculated as $e_i = h_{fi}^0 + \int_{T_R}^T C_{pi} dT - R_u T$ where MW_i , C_i , C_{pi} and h_{fi}^0 expressed as the molecular weight, mass concentration, specific heat at constant pressure and heat of formation respectively. Apart from this, R_u called as universal gas constant, T_R as character reference temperature and 'N' denotes number of species. In the present case, utilizes Venkat Krishnan limiter to provide second order accuracy. The solver is incorporated by higher order reacting convective or inviscid fluxes, AUSM scheme.

3. VALIDATION

A present finite-rate chemistry model includes eight species N₂, NO, O₂, CO₂, C, O, CO and N and ten elementary chemical reactions. The rate coefficient and chemical reactions used in non-equilibrium conditions are mentioned in Table 1.97% CO₂ and 3% N₂ is considered for non-reacted freestream flow. The following reactions accord with rate constants have being studied by Macieland Pimenta for the chemical non-equilibrium around Martian atmospheric conditions.

Table 1. Rate-Coefficients and Chemical Reactions used in non-equilibrium

Sl No	Chemical Reaction	$K_{bi} (cm^3mole^{-1}se)$	$K_{fi}(cm^3mole^{-1}se)$
1	$M + N_2 \rightarrow 2N + M$	$1.5 \times 10^{18} T^{-1.0}$	$2.5 \times 10^{19} T^{-1.0} e^{-1.132 \times 10^5 / T}$
2	$NO + M \rightarrow N + O + M$	$3.5 \times 10^{18} T^{-1.0}$	$4.1 \times 10^{18} T^{-1.0} e^{-7.533 \times 10^4 / T}$
3	$CO + O \rightarrow C + O_2$	$9.4 \times 10^{12} T^{0.25}$	$2.7 \times 10^{12} T^{0.5} e^{-6.945 \times 10^4 / T}$
4	$CO + N \rightarrow NO + C$	$2.6 \times 10^{10} T^{0.5}$	$2.9 \times 10^{11} T^{0.5} e^{-5.363 \times 10^4 / T}$
5	$NO + O \rightarrow O_2 + N$	$9.5 \times 10^9 T^{1.0}$	$3.0 \times 10^{11} T^{0.5} e^{-1.946 \times 10^4 / T}$
6	$CO + M \rightarrow C + O + M$	$1.0 \times 10^{18} T^{-1.0}$	$4.5 \times 10^{19} T^{-1.0} e^{-1.289 \times 10^5 / T}$
7	$CO_2 + O \rightarrow CO + O_2$	$2.5 \times 10^{12} e^{-2.4 \times 10^4}$	$1.7 \times 10^{13} e^{-2.65 \times 10^4 / T}$
8	$N_2 + O \rightarrow NO + N$	$1.6 \times 10^{11} T^{0.5}$	$7.4 \times 10^{11} T^{-0.5} e^{-3.79 \times 10^4 / T}$
9	$CO_2 + M \rightarrow CO + O + M$	$2.4 \times 10^{15} e^{-2.184 \times 10^3 / T}$	$3.7 \times 10^{14} e^{-5.25 \times 10^4 / T}$
10	$O_2 + M \rightarrow 2O + M$	$9.1 \times 10^{15} T^{-0.5}$	$9.1 \times 10^{18} T^{1.0} e^{-5.937 \times 10^4 / T}$

Numerical tests have been conducted to validate the accuracy of the present formulation. The test cases include sphere of diameter 25.4mm and ramp angles at 10 and 15 degree are implemented to validate the developed solver.

3.1 Flow Through Ramp

In the computational solution, the geometry 2D ramp of angle 10 degree and 20 degree for the following Mach 4 and 5. Further freestream conditions includes pressure of 199.45Pa and temperature of 131.70 K with mesh size of 280x150. The Mach contour attained are shown in fig.1. to fig.4. With the purpose of authenticating the solver, pressure and temperature ratios along with shock wave angle (β) are compared with the analytic predictions used for low enthalpy test conditions. The comparisons have been discussed in detail and tabulated. By studying table 2, it can be observed that the developed solver provides satisfactory result at low enthalpy conditions.

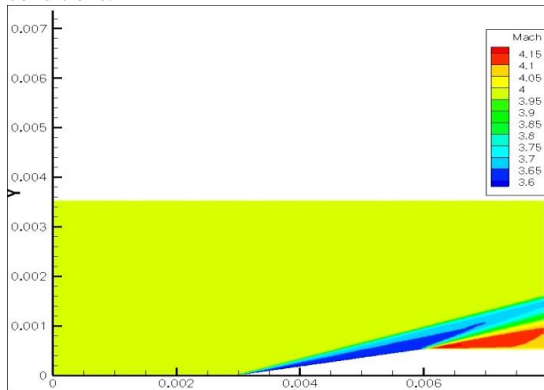


Figure 1. Ramp angle of 10° at Mach 4

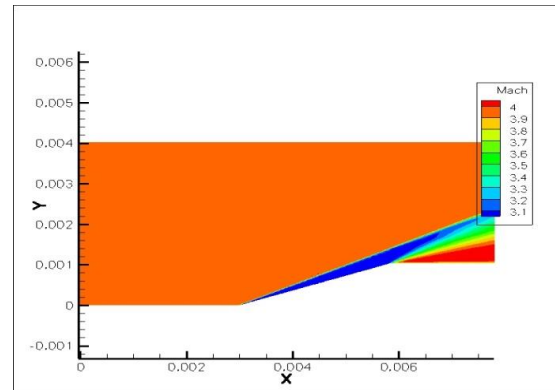


Figure 2. Ramp angle of 20° at Mach 4

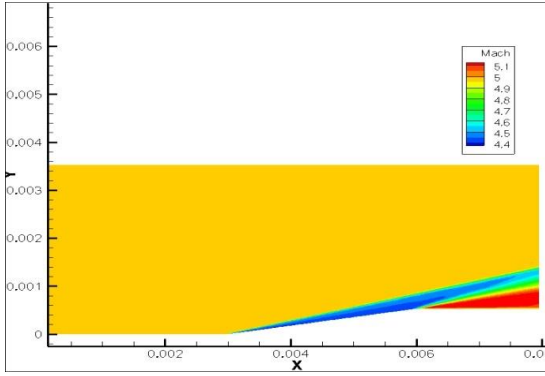


Figure3. Ramp angle of 10° at Mach 5

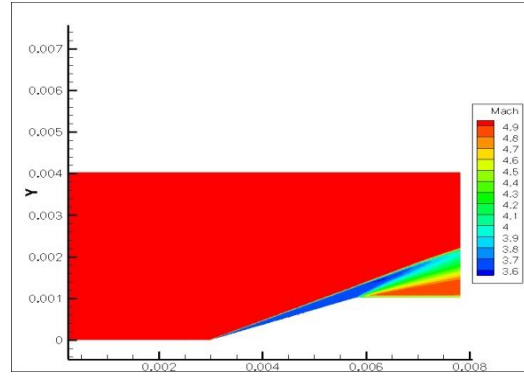


Figure4. Ramp angle of 20° at Mach 5

Table 2. Comparison of in-house solver and Analytical values at different ramp angle- Mars conditions

Ramp Angle.	Mach No.	Pressure ratio		Temperature Ratio		Shock Wave angle (β)	
		Analytical	Solver	Analytical	Solver	Analytical	Solver
10	4	2.373	2.477	1.241	1.229	21.840	19.971
	5	2.850	2.973	1.312	1.288	18.976	17.949
20	4	4.782	5.175	1.580	1.476	31.411	32.780
	5	6.410	6.894	1.799	1.639	28.757	28.9612

3.1 Flow over Sphere

Simulations are conducted for flow of carbon dioxide (CO₂) across a sphere of 25.4mm diameter in order to justify the current solver for reacting flow situations. Two test cases of velocity 4.220km/s plus 2.845km/s have been discussed here.

Table 3. Test Conditions and Result Comparisons of flow over sphere 25.4mm

Sphere Diameter(mm)	Velocity(km/s)	Ambient Temperature(K)	Ambient Pressure (Kpa)	Shock Stand of distance	
				Analytical	Solver
25.4	4.220	293.7	2.420	0.14493	0.11633
	2.845	293.2	7.425	0.14728	0.11811

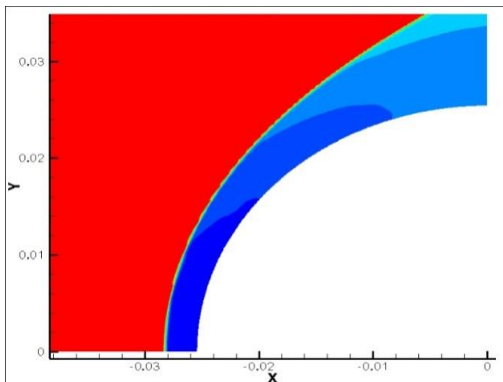


Figure5. Bow Shock wave at 4.220km/s

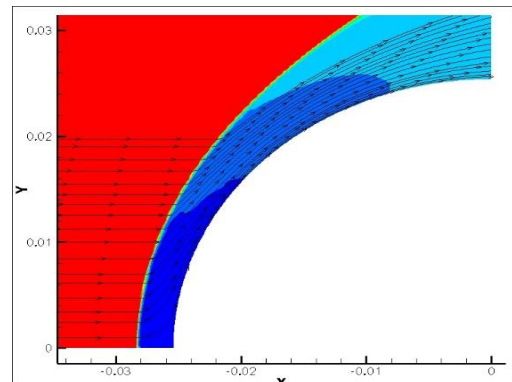


Figure6. Streamline at 4.220km/s

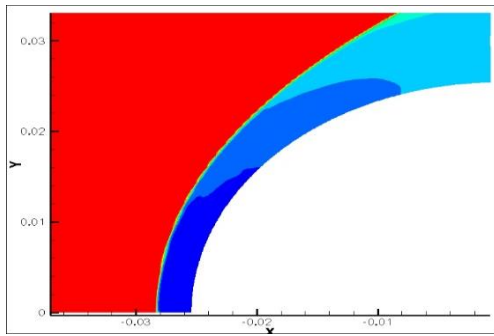


Figure7. Bow Shock wave at 2.845km/s

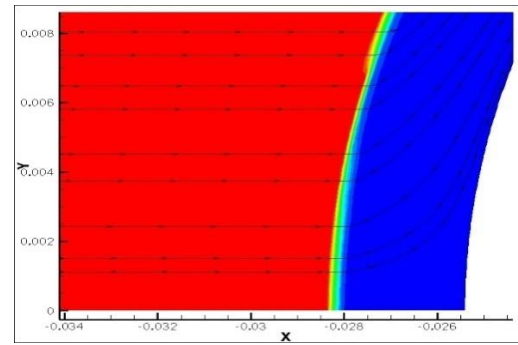


Figure8. Streamline at 2.845km/s

The details of the test condition are shown in table 3. In the table, shock standoff distance calculated is compared with in house solver. Fig 5 till fig.8 shows bow shock wave at two different velocities. It is noticeable from the table that the shock stand-off distance at two freestream velocities shows minor changes.

Reference: -

1. M. Sharma, A. B. Swantek, W. Flaherty, J. M. Austin, S. Doraiswamy, G. V. Candler, Experimental and numerical investigations of hypervelocity carbon dioxide flow over blunt bodies, *Journal of Thermophysics and Heat Transfer* 24 (2010) 673– 683.
2. Rodrigo C. Palharini, Craig White, Thomas J. Scanlon, Richard E. Brown, Matthew K. Borg, Jason M. Reese, Benchmark numerical simulations of rarefield non-reacting gas flows using an open-source DSMC code, *Computers and Fluids* (2015), doi: 10.1016/j.compfluid.2015.07.021.
3. Mahsa Mortazavi, Doyle Knight Olga Azarova, Jingchang Shi and Hong Yan, Numerical Simulation of Energy Deposition in a Supersonic Flow Past a Hemisphere, 52nd Aerospace Sciences Meeting AIAA 2014-0944.
4. R. A. Mitcheltree, P. A. Gnoffo, Wake flow about a MESUR mars entry vehicle, 6th Joint Thermophysics and Heat Transfer Conference, Fluid Dynamics and Colocated Conferences, Colorado Springs, CO, U.S.A., 1994.
5. Dongjun Liao, Sen Liu, Hexiang Jian, AiminXie, ZonghaoWang andJie Huang, Measurement and Calculation of Shock Stand-off Distances over Hypersonic Spheres in CO₂, *International Space Planes and Hypersonic Systems and Technologies Conferences*, 21st AIAA International Space Planes and Hypersonics Technologies Conference
6. R.B. Kudenatti, B. Jyothi, Two-dimensional boundary-layer flow and heat transfer over a wedge: numerical and asymptotic solutions, *Thermal Science and Engineering Progress* (2019), doi: <https://doi.org/10.1016/j.tsep.2019.03.006>
7. K. Satheesh and G. Jagadeesh, Effect of concentrated energy deposition on the aerodynamic drag of a blunt body in hypersonic flow *PHYSICS OF FLUIDS* 19, 2007 American Institute of Physics. DOI: 10.1063/1.2565663.
8. Huang Fei, Jin Xu-hong, Lv Jun-ming, and Cheng Xiao-li, Impact of Martian atmosphere parameter uncertainties on entry vehicles aerodynamic for hypersonic rarefied conditions, *AIP Conference Proceedings* 1786, 190006 (2016); doi: 10.1063/1.4967684
9. Robert d. Braun, robert m. Manning, mars exploration entry, descent, and landing challenges, *Journal of Spacecraft and Rockets*, vol. 44, no. 2, March–April 2007, doi: 10.2514/1.25116
10. J.D. Anderson, *Modern Compressible Flow: with Historical Perspective*, second ed., McGraw-Hill, 1990.